

Anisotropic full azimuth velocity model building using Joint Reflection-Refraction tomography

Matan Shustak*, Itai Sharabi, Orly Kletenik-Edelman, Elive Menyoli, Ike Imala, Ronit Levy and Zvi Koren,
Emerson

Summary

One of the main challenges in seismic imaging, especially of land data, is building the near surface velocity model, as it is normally characterized by very low velocity values with different types of local anomalies. Resolving the near surface velocity model using only refraction data (e.g., refraction tomography) is insufficient, as it does not provide the required lateral resolution. Using only reflection data is equally insufficient, as it does not provide the required vertical resolution. We present a tomographic approach for simultaneously resolving the shallow and deep subsurface anisotropic velocity fields, where we jointly utilize both reflection and refraction data. By constructing a constrained joint reflection-refraction objective function, we show that this tomography can provide high-resolution anisotropic velocity models and subsequent accurate depth migration images. The method has been successfully applied to a 3D dataset from the Eagle Ford play in south central Texas. The results demonstrate that the method produces a very accurate near surface anisotropic velocity model.

Introduction

A particular challenge in land seismic exploration is determining the velocity heterogeneity and anisotropy effects on the near-surface model, in particular below rough topography. The near surface velocity field normally involves extremely low velocities which rapidly grow with depth, small scale anomalies, buried channels/rivers, etc. The dataset used in this study represents such a complex land environment: It was acquired in 2009 in the Eagle Ford play in Live Oak County in south central Texas, covering an area of 130 square miles. The topography of the area is moderately hilly, with elevations ranging from 192ft to 443ft and eroded by meandering river systems (Figure 1). The near surface sediments are composed of unconsolidated alternating beds of sand, silt, clay, and gravel from alluvial deposits (Anders and Baker 1961). The base of the weathered zone, which extends to about 3000ft, is covered mainly by a fluvial conglomerate. The alternating geology introduces rapid lateral velocity variation into this shallow section. Our study shows that in this type of near surface geology, seismic gather flattening and the corresponding final image are considerably improved using a Joint Reflection-Refraction (JRR) tomographic inversion applied simultaneously to the shallow and deeper parts of the model.

The traditional approach to estimating the velocity model for land surveys involves first the application of refraction

tomography to derive the near-surface velocity model. This is followed by applying reflection tomography to invert for the deeper subsurface model (Jun et al., 2018). However, with this approach, the remaining (unresolved) shallow velocity errors negatively affect the estimated velocity in the deeper parts and the corresponding seismic images. In addition, without adding proper constraints, the already resolved shallow model might be blurred and deteriorated by the reflection information. The proposed JRR tomography makes it possible to invert for consistent and plausible velocity models by simultaneously minimizing the traveltime errors of both reflection and refraction data.

Refraction waves mainly propagate laterally and thus provide high vertical velocity resolution along the propagating areas. On the other hand, reflection waves mainly propagate vertically, providing high velocity resolution in the lateral direction (Panizzardi et al., 2012). Compared to the conventional workflow, we show that combining the different characteristics of the refraction and reflection waves and their inherent different directivity resolution within the JRR tomography, results in higher accuracy and higher resolution of the anisotropic velocity fields across the whole subsurface section.

In this paper we compare the proposed joint tomographic workflow with the conventional reflection-only tomographic solution, by analyzing the velocity volumes, image gathers, final images, and the traveltime error statistics.

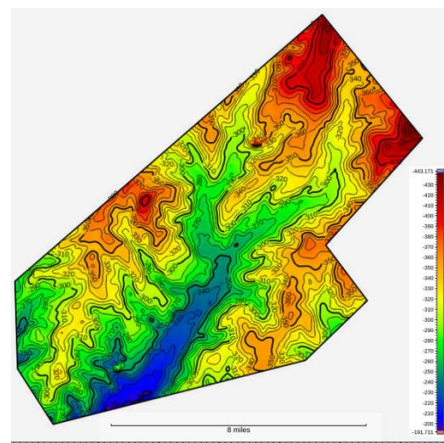


Figure 1. Topography map of the Eagle Ford Play in Live Oak County in south central Texas

Full azimuth Reflection-Refraction tomography

Method

The proposed JRR objective function aims to minimize the traveltime errors of both the first arrivals for the refraction data, and the residual moveouts which were automatically picked along full azimuth reflection angle domain depth common image gathers (CIGs),

$$\min_{\delta m} \left(\begin{bmatrix} s_{rfr} \\ s_{rfl} \end{bmatrix}^T \left(\begin{bmatrix} \frac{\partial G_{rfr}}{\partial m_{rfr}} & \frac{\partial G_{rfl}}{\partial m_{rfl}} \end{bmatrix} \begin{bmatrix} \delta m_{rfr} \\ \delta m_{rfl} \end{bmatrix} - \begin{bmatrix} \delta t_{rfr} \\ \delta t_{rfl} \end{bmatrix} \right) \right)^2, \quad (1)$$

where δm is the perturbations vector of the axial slowness, and the Thomsen delta and epsilon parameters ($\delta s, \delta \delta, \delta \epsilon$) for both the refraction and reflection rays (rfr, rfl). $\frac{\partial G}{\partial m}$ are the Hamiltonian derivatives matrix with respect to the parameter perturbations. The vector s represents the scaling factors assigned to each ray and δt is the traveltime errors

(Figure 2). The initial inputs for both workflows were derived from a prior isotropic refraction tomography and extracted well information of the anisotropic parameters: Thomsen delta, and epsilon (Figure 2). The imaging method used in this study is the full-azimuth angle domain migration (Koren and Ravve 2011) applied to the VTI model

After running both the conventional reflection tomography and the JRR tomography, significant differences in the shallow subsurface can be seen between the results of both workflows. The JRR tomographic results are characterized by higher resolution, yielding more details in the shallow subsurface and subsequently a more plausible deeper part, following the geological trend (Figure 3).

A further observation of the different tomography models may be seen by overlaying the Thomsen epsilon model of

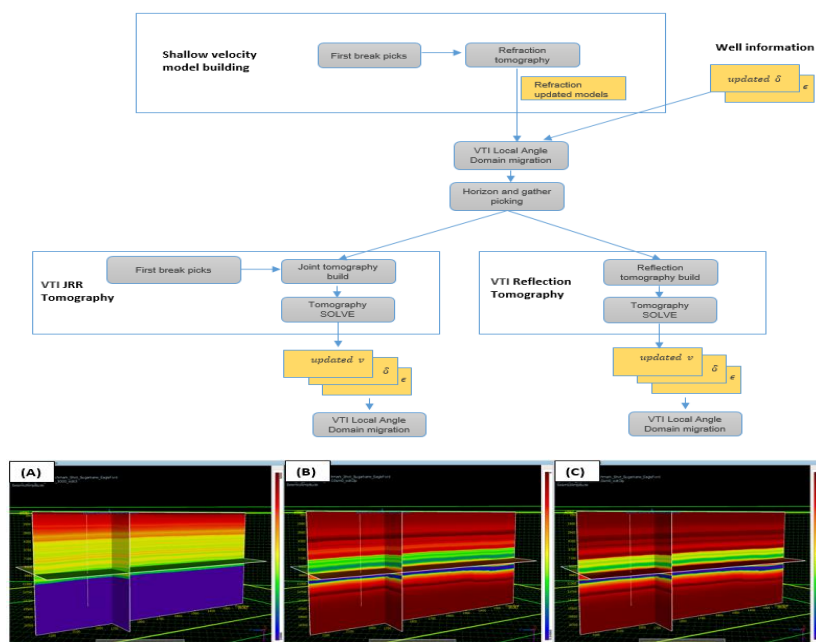


Figure 2. Top: Illustration of the comparison workflows Reflection Tomography and Reflection-Refraction Tomography. Bottom: Initial velocity model (A), initial delta (B) and initial epsilon (C).

along the rays for each of the wave modes. The scaled joint objective function makes it possible to properly balance between the two different (refraction and reflection) phenomena for building a detailed and reliable model. The solution is constructed using a global approach, thus retrieving information regarding the shallow and deep sections simultaneously

Example

This study compares two workflows: that of conventional reflection tomography and the proposed JRR tomography

both solutions on the initial stack image. This comparison shows a significant difference in the shallow part while the reflection data input is the same for both workflows. The JRR tomographic solution for the Thomsen epsilon structure in the shallow terrain is considerably more detailed. Moreover, the Thomsen epsilon model produced by the JRR solution aligns much better with the layers along the stack image. Figure 4 illustrates how the JRR results follow the image reflectivity structure in the shallow section, while the reflection tomography offers a smoother and less detailed solution.

Full azimuth Reflection-Refraction tomography

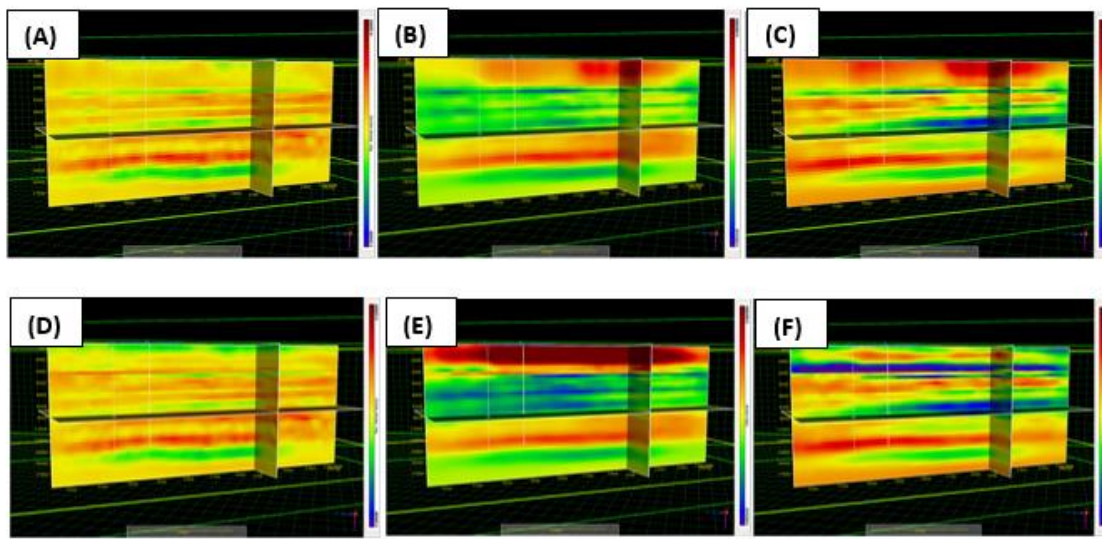


Figure 3. Output residual volumes from both workflows. Upper row, results of conventional reflection tomography - residual velocity (A), residual delta (B), residual epsilon (C). Lower row, JRR tomography - residual velocity (D), residual delta (E), residual epsilon (F).

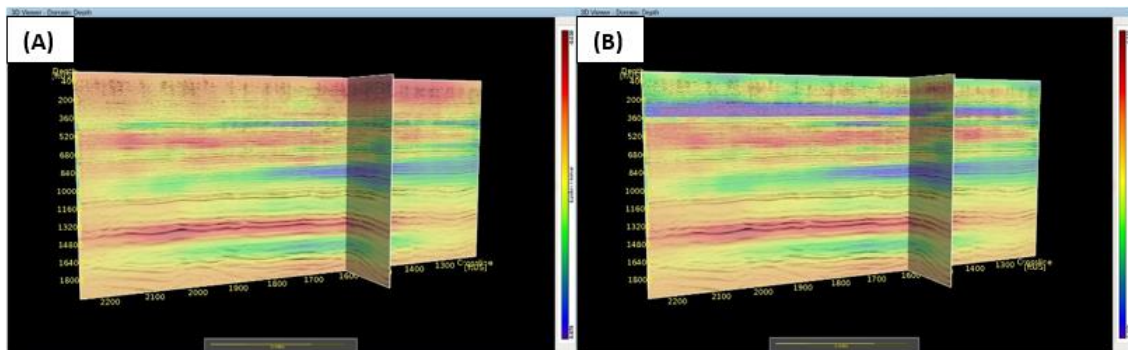


Figure 4. Residual epsilon laid on stack section from conventional reflection tomography (A), JRR tomography (B).

In the next step of the workflow, we used the output of both the reflection and the JRR tomographic solutions as input to another migration iteration. The analysis of both images and the flatness of the events along the CIGs were used to verify the models' reliability and correctness. Both models yielded flat events in the deeper part. However, the JRR-based migrated events at the shallow to mid-part of the model were flatter and more coherent. In addition, a new event appears in the shallow section and especially improved long angles gather flatness and image quality in both the shallow and deeper parts of the model (Figure 5).

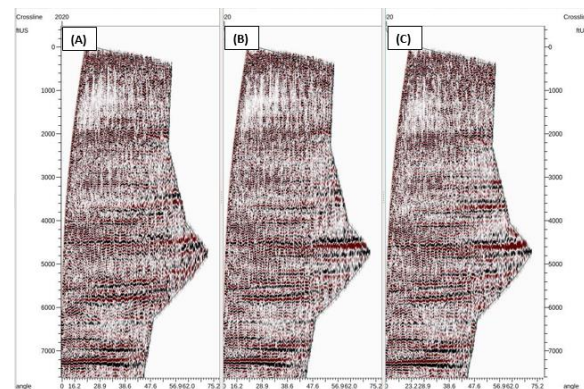


Figure 5. Prestack local angle domain CIGs (common image gathers). Imaging using initial velocity (A), reflection tomography output model (B) and JRR tomography output model (C).

Full azimuth Reflection-Refraction tomography

A convergence study was performed for further statistical analysis in order to verify the correctness and reliability of the models. Since the objective function minimizes the traveltime errors of both reflection and refraction data, studying the errors is a good measure of the convergence quality and suitability of the model to the data. The reflection errors are manifested in the relative residual moveouts which measure the ratio between the moveout at wide angles to the zero-offset depth. The refraction errors are measured by averaging the absolute relative difference between the modeled and observed traveltimes for all receivers per a source location.

Figure 6A illustrates the initial relative traveltime errors for both wave types. The initial refraction relative traveltime errors range between 7-9%, while the reflection errors range between 2-3%. Figure 6B shows the relative traveltime errors of the reflection tomography workflow. The refraction errors increased to 8-11% and converged for the reflection data to 1-2%, where the reduction of the reflection data errors indicates that the gathers were flattened in depth. However, the increase in errors in the refraction rays shows that the solution in the shallow to mid-shallow subsurface deteriorated. Figure 6C illustrates the residual errors of the JRR data. The results show a more complete solution, while the errors converge to 1-2% for both refraction and reflection waves. This is strong evidence for the need to combine information from both refraction and reflection data types to minimize errors throughout the entire depth range.

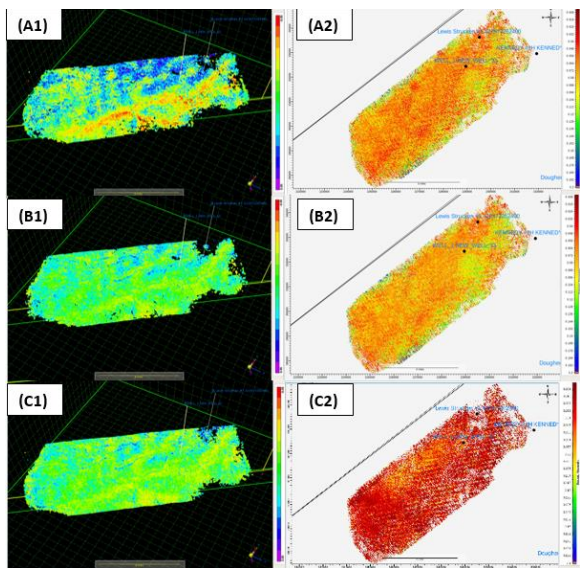


Figure 6. Remaining relative traveltime errors. Initial model reflection at 7000ft (A1) refraction (A2). After reflection tomography at 7000ft (B1) refraction (B2). After JRR tomography at 7000ft (C1) refraction (C3).

Conclusions

This work demonstrates the benefits of jointly inverting reflection and refraction traveltime errors to simultaneously estimate shallow and deeper velocity models in a land environment for improving seismic imaging. The integration of the two data types offers a complete solution by evenly minimizing the residual errors. When using only the reflection data approach, the shallow velocity parameters from refraction tomography are not preserved. In the joint workflow, a more consistent and accurate anisotropic inversion (in particular for the Thomsen epsilon parameter) is observed in the shallow regions. This certainly improves the long angles gather flatness and image quality in both the shallow and deeper parts of the model.

Joining the reflection and refraction data improves the resolution of the velocity parameters in both horizontal and vertical directions. In this case study example, the higher resolution velocity model uncovered new events that could not previously be observed using a conventional workflow.

Acknowledgments

The authors would like to thank Shiv Singh for his valuable contribution processing the initial velocity model and for fruitful discussion. We also thank Seitel for release of the material for publication.

REFERENCES

- Anders, R. B., and E. T. Baker Jr, 1961, Ground-water geology of live oak county, Texas: Bulletin 6105 Prepared in cooperation with the Geological Survey United States Department of the Interior and Live Oak County
- Jun, T., P. Gengxin, J. Jiao, G. Yan, and X. Zhu, 2018, Integrated turning-ray and reflection tomography for velocity model building in foothill areas: Interpretation, **6**, no. 4, SM63–SM70, doi: <https://doi.org/10.1190/INT-2018-0005.1>.
- Koren, Z., and I. Ravve, 2011, Full-azimuth subsurface angle domain wavefield decomposition and imaging Part I: Directional and reflection image gathers: Geophysics, **76**, no. 1, S1–S13, doi: <https://doi.org/10.1190/1.3511352>.
- Panizzardi, J., and N. Bienati, 2012, Null space of joint reflection and diving ray tomography in TI media: SEG Technical Program Expanded Abstracts 2012, doi: <https://doi.org/10.1190/segam2012-1070.1>.
- Ravve, I., and Z. Koren, 2011, Full-azimuth subsurface angle domain wavefield decomposition and imaging: Part 2—Local angle domain: Geophysics, **76**, no. 2, S51–S64, doi: <https://doi.org/10.1190/1.3549742>.